Cancer Immunology, Immunotherapy (2023) 72:1673–1683
https://doi.org/10.1007/s00262-022-03355-6

RESEARCH

A nanotherapeutic system for gastric cancer suppression by synergistic chemotherapy and immunotherapy based on iPSCs and DCs exosomes

Yezhou Li[3] · Leilei Tian[4] · Tiancheng Zhao[2] · Jiayu Zhang[1]

Received: 3 July 2022 / Accepted: 21 December 2022 / Published online: 9 January 2023

Abstract

Background Chemotherapeutic drugs, the indispensable therapy in the treatment of gastric cancer, contain many problems such as high organ toxicity and insufficient therapeutic effect. The development of nanodrug delivery carriers with both tumor targeting function and immune stimulation ability possesses the potential to remedy these practical defects.

Methods and results In this study, a tumor targeting nanosystem that combines chemotherapy with immunotherapy was applied to the treatment and prognosis of gastric cancer. The fusion vector of iPSCs and DCs exosomes, which simultaneously possess the ability of tumor targeting and immune factor recruitment, effectively improved the in vivo efficacy of chemotherapy drugs and released the suppressed T lymphocytes under the action of modified PD-1 antibody to dredge the immunotherapy process. In addition, extensive recruitment of immune cells to clean the environment while exposing vast tumor antigens efficiently amplified the anti-tumor immune effect and ensured the good prognosis.

Conclusions Nanodrug delivery system DOX@aiPS-DCexo could effectively inhibit the expansion process of gastric cancer MFC through synergistic chemotherapy and immunotherapy and demonstrated the capacity of improving prognosis.

Graphical Abstract

Scheme: schematic illustration of the nanostructure DOX@aiPS-DCexo and the mechanism of action.

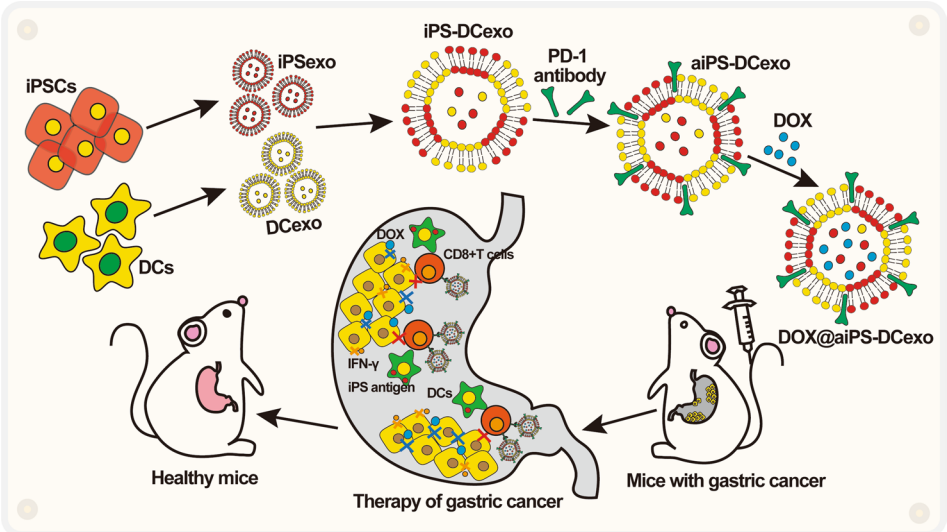

Keywords Gastric cancer · iPSCs exosomes · DOX · Immune therapy · Synergistic treatment

Extended author information available on the last page of the article

Abbreviations

5-FU	Fluorouracil
aPD-1	Programmed cell death protein 1 antibody
iPSCs	Induced pluripotent stem cells
DCs	Dendritic cells
DOX	Doxorubicin
BMDCs	Mouse bone marrow-derived dendritic cells
GCSC	Gastric cancer stem cells
TEM	Transmission electron microscopy
DLS	Dynamic light scattering
DMEM	Dulbecco's modified eagle medium
FBS	Fetal bovine serum
ELISA	Enzyme-linked immunosorbent assay
PMSF	Phenylmethylsulfonyl fluoride
H&E	Hematoxylin and eosin
IVIS	In vivo imaging instruments

Introduction

Gastric cancer has become one of the most malignant tumors that seriously threaten human health and patients' quality of life due to its characteristics of insidious symptoms, short course, rapid development, early metastasis and relatively poor prognosis of disease [1–4]. Surgical treatment, radiotherapy, chemotherapy and immunotherapy were commonly used in clinical treatment. Chemotherapy drugs, such as mitomycin, cisplatin, adriamycin and fluorouracil (5-FU), are the most appropriate treatment of advanced unresectable tumors for directly and effectively damage tumor tissue [5–7]. However, it can only shrink the tumor coverage and cannot completely remove tumor substances, resulting in a poor prognosis [8, 9]. Moreover, the lack of tumor tissue targeting, low efficacy and normal tissue toxicity of chemotherapy drugs seriously affects the quality of life of patient. Therefore, the development of accurate delivery vectors for chemotherapy drugs with tumor tissue targeting and well biocompatibility will be the research direction to improve their drug formation [10–12].

Pembrolizumab, an effective PD-1 inhibitor for advanced esophageal gastric cancer with positive expression of PD-1 ligand, has become the first anti-PD-1 drug to be approved in the USA, ushering in an era of monoclonal antibody immune checkpoint inhibitor therapy toward clinical immunotherapy for gastric cancer [13–15]. However, the effect of aPD-1 alone is not enough to abundantly recruit immune cells to infiltrate tumors, so it is necessary to combine immunoadjuvant and other treatments to expand the efficacy of immunotherapy [13, 16–18].

As the drug carriers with both functional therapeutic and targeted delivery capacity, multiple exosomes have been proved to effectively improve the therapeutic effect of drugs. Among them, exosomes of induced pluripotent stem cells (iPSCs) (iPSC-exos) have been confirmed to possess the tumor tissue targeted ability mediated by the CXCR4/SDR1 axis [19–22], and they could also inhibit the regeneration of gastric cancer stem cells (GCSC) for the varieties contents such as serum albumin, keratin fiber binding protein trichoplein, cell transcription inhibitor protein Zbtb4, CDC14A and so on [23–25]. Exosomes of dendritic cells (DC-exos) can stimulate the mature differentiation of antigen-presenting cells by regulating NF-κB pathways, recruit downstream lymphocytes to infiltrate tumor tissues and reshape the tumor immune microenvironment [26–30]. However, the simplex biological function and insufficient loading efficiency of single exosomes limited their application as functional drug delivery vectors [31–34]. Therefore, by fusing iPSC-exos with DC-exos, the fusion drug delivery vector iPS-DCexo can not only increase the uploading ability of anti-tumor drugs, but also retain biological functions such as tumor tissue targeting, tumor inhibition and immune stimulation. At the same time, PD-1 antibody was utilized to modified the fusion carrier for relieving the immunosuppression of lymphocytes in tumor tissues and enhancing the efficacy of immunotherapy [35–38]. After the package of chemotherapy drug doxorubicin (DOX), the converged system DOX@aiPS-DCexo could target and damage tumor tissues and awake and amplify a series of anti-tumor immune responses, realizing the synergistic treatment of chemotherapy and immunotherapy [39–41].

In this study, we reported a tumor-killing system DOX@aiPS-DCexo based on modified iPSC-exos and DC-exos fusion vector for the transport of chemotherapeutic drugs DOX. After injection into the body, it can target the destruction of gastric tumor tissue, expose a large number of tumor-related antigens, inhibit the regeneration and tissue remodeling of gastric cancer stem cells, further kill and entirely remove tumor-related substances through the immune cells recruitment, achieving the goal of effectively tumor inhibition in growth, metastasis and recurrence and reversing the infaust prognosis of existing gastric cancer treatment methods. Combined with the advantages in availability of raw materials, well biocompatibility and low toxicity of normal tissues, the system owns the potential of clinical application in cancer therapy.

Methods

Cells

All cell lines used in the experiment were purchased from American Type Culture Collection (ATCC, Shanghai) and preserved in the China-Japan Union Hospital of Jilin University. Before use, consistency was compared according to the cell morphology and cell growth properties guided by the ATCC

website to ensure that no variation occurred. Cells besides iPSCs were cultured in Dulbecco's modified eagle medium (DMEM high glucose, Keygenbio, cat no. KGM12800H-500) containing 10% fetal bovine serum (FBS, Thermo Fisher, cat no. 10099-141), and iPSCs were cultured in the ncTarget hPSC Medium (donated by China Pharmaceutical University and purchased from Nuwacell Biotechnologies Co., Ltd, cat no. RP01020). All cells were maintained in the environment at 37 °C and 5% CO_2.

The marrow cavities of femurs and tibias of mice were dissected for obtain mouse bone marrow-derived dendritic cells (BMDCs) and the cultivate BMDCs in the lower chamber of transwell plates with DMEM containing 10 ng/mL GM-CSF (MedChemExpress, cat no. HY-P7361) and 5 ng/mL IL-4 (MedChemExpress, cat no. HY-P70653) for 7 days.

Animals

ICR, BALB/c mice (6–8 weeks) were purchased from Jilin University. ICR mice were used to analysis distribution, and BALB/c mice were to construct the tumor model. Mice were treated under protocols approved by the Institutional Animal Care and Use Committee.

Extraction of exosomes

After the cells were cultured continuously to a stable state, the culture medium was collected for 3 consecutive days and centrifuged at a low speed of 300× g for 10 min. Living cells and large cell fragments in the precipitation were discarded. Then, the supernatant was centrifuged at 2000× g for 10 min, and the precipitated dead cells were discarded. The supernatant was continued for 10,000× g for 30 min to remove the cell debris and obtain the cultured liquid. The cultured liquid was centrifuged at 100,000× g centrifugal force for 70 min and then, resuspended precipitation with PBS and centrifuged again at 100,000× g for 70 min to obtain pure exosomes.

SDS-page and Western blot

All proteins were extracted in RIPA (Beyotime, cat no. P0013D) and PMSF (Beyotime, cat no. ST505), prepared in loading buffer and measured by BCA kit (Beyotime, cat no. P0012S). The samples were heated to 95 °C and kept for 10 min, and the same concentration of each groups was loaded in the SDS polyacrylamide gel. After running at 80 V for 30 min and 120 V for 90 min, protein was removed to the PVDF membrane at 200 mA for 90 min. In Fig. 1F, aPD-1 was captured by the Streptavidin-HRP (Beyotime, cat no. A0305).

Preparation and characterizations of fusion carrier

The fusion carrier was prepared by ultrasonic extrusion. iPSCs exosomes and DCs exosomes were mixed at a ratio of 3:2 and completely suspended in an ice water bath. After 30 min of ultrasonic treatment with 100 w, the system was placed in a 37 °C water bath to oscillate for 1 h. The fusion carriers were extruded 20 times and 20 times at 400 nm and 200 nm, respectively, by liposome extruder.

To demonstrate the successful preparation of fusion vectors, two types of exosomes were labeled with fluorescent cell membrane probes DiO (Beyotime, cat no. C1038) and DiI (Beyotime, cat no. C1036), respectively, before fusion. Flow cytometry analysis was used to observe the overlap of fluorescence signals after direct mixing or fusion operations.

Modification of fusion vector by PD-1 antibody

The modification of PD-1 antibody (ProteinTech, cat no. 18106–1-AP) was applied via streptavidin–biotin method. Firstly, PD-1 antibody was coupled with biotin-PEG_{3500}-NHS (Peng sheng Biological, Shanghai) to generate biotin-PEG3500-aPD-1, and the binding ability of biotin-labeled antibodies was investigated at different antigen envelope concentrations. After coated with different concentrations of PD-1 antigen, the plate was sealed with 1% BSA (Beyotime, cat no. ST2249). Then, 100 µl biotin-labeled antibody with working concentration of 1 : 1000 was added to each well. Streptavidin-HRP (Beyotime, cat no. A0305) was used for color development. After washing, TMB (Beyotime, cat no. ST746) substrate system was added to measure the OD value at 450 nm.

Meanwhile, the fusion vector was incubated with streptavidin-PEG_{3500}-DSPE (Peng sheng Biological, Shanghai) in 37 °C water bath for 30 min. Streptavidin-fusion vector was co-incubated with biotin-aPD-1 for 30 min to obtain aPD-1-modified fusion vector aiPS-DCexo, and the validation of the modification was proved by Western blot.

Preparation of the nanosystem DOX@aiPS-DCexo

DOX was uploaded by ultrasonic-mechanical co-extrusion method. In short, the fusion vectors generated above were co-incubated with DOX at 37 °C water bath for 1 h and then, co-incubated with DOX at 50 w, 37 °C water bath ultrasonic environment for 20 min to promote the close binding of DOX to the fusion vectors aiPS-DCexo. The mixture was repeatedly extruded by the liposome extruder through the 200 nm membrane five times and the 100 nm membrane five times, respectively, to generate the nanosystem DOX@aiPS-DCexo under mechanical forces.

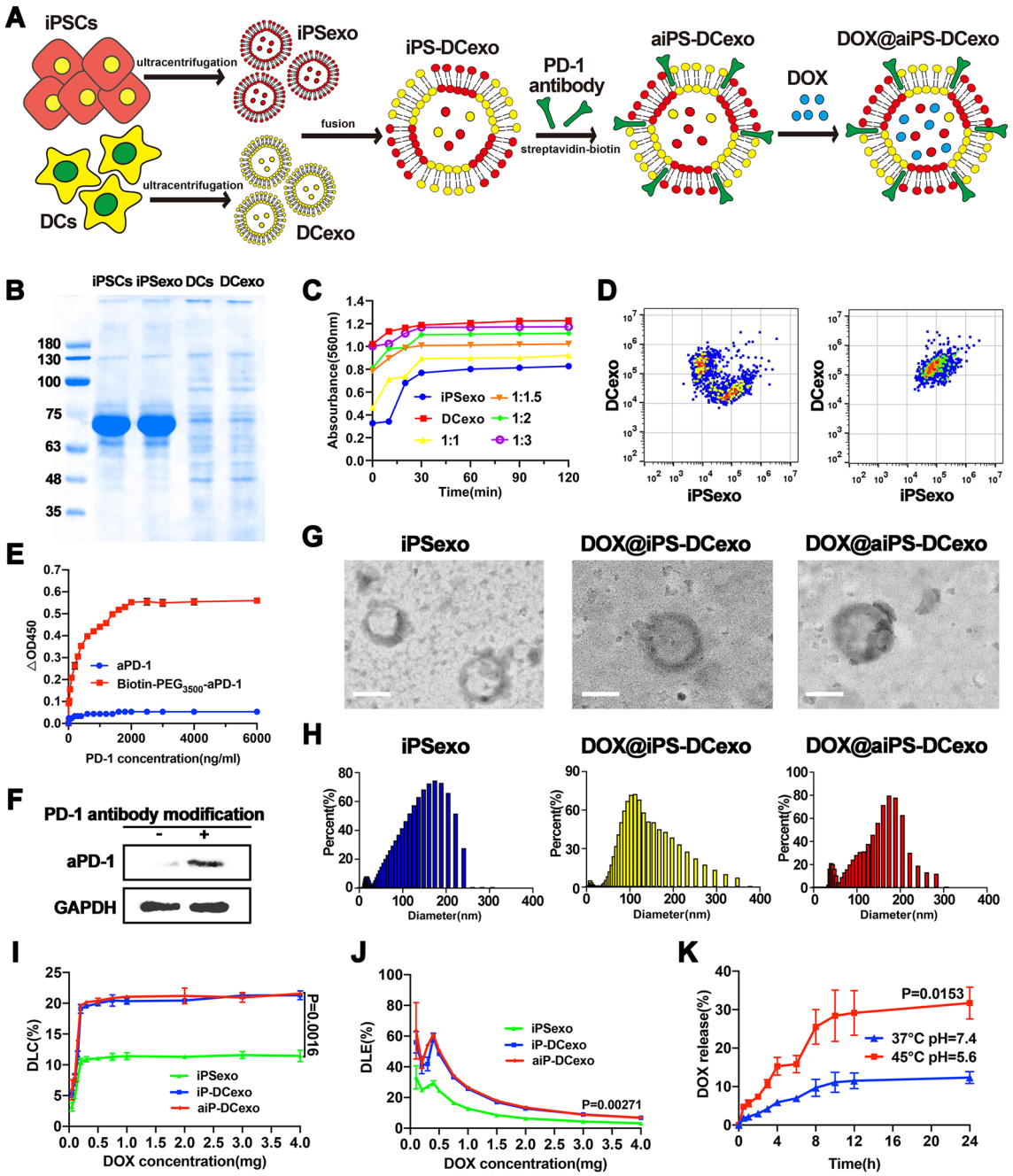

Fig. 1 Construction and characterization of nanosystems DOX@aiPS-DCexo. **A** Scheme of the preparation of DOX@aiPS-DCexo. **B** SDS-PAGE protein analysis of the whole protein expression in iPSCs, DCs, iPSCs exosomes and DCs exosomes. **C** Determination of optimal fusion ratio of two exosomes. **D** Flow cytometry analyzer of the fusion of the two nanoparticles. **E** OD values at 450 nm in different concentrations antigen coated plates. **F** WB analysis of vector-modified PD-1 antibody. **G** Transmission electron microscopy (TEM) observation of the surface morphology of DOX@aiPS-DCexo. Scale bars are 100 nm. **H** DLS analysis of particle size distribution of nanosystem DOX@aiPS-DCexo. Encapsulation rate (**I**), drug loading capacity (**J**) and drug release (**K**) of the nanosystem DOX@aiPS-DCexo. All data were expressed as mean ± SD. Statistical significance was calculated by one-way ANOVA with Tukey's post hoc test

Encapsulation rate, drug loading capacity and drug release of fusion carrier

DOX loading capacities of iPS-exo, iPS-DCexo and aiPS-DCexo were demonstrated by drug loading capacity and drug loading efficiency.

Drug loading capacity = mass of actual drug encapsulation/mass of (actual drug encapsulation + polymer) × 100%

Drug loading efficiency = mass of actual drug encapsulation/mass of theoretical drug encapsulation × 100%

The drug release curve was measured by dialysis. Phosphate buffers with different pH values were used as release media. 1 ml of peripheral buffer was taken at the set time point, and the same amount of blank buffer was added in time. DOX content in all solution samples collected was detected under the same experimental conditions.

Uptake by macrophage RAW264.7

DOX in all groups was fluorescently labeled with rhodamine B. The cell line Raw264.7 was randomized to investigate cell uptake when cultured to 80% in DMEM high glucose medium. After changing the fresh medium for 12 h, particles with the same fluorescence amount were added and contained the culture environment for 4 h. DAPI labeled nuclei were added into the confocal dish 10 min before imaging.

Transwell

The Transwell system was divided into two chambers, in which MFC cells were cultured in the upper chamber and BMDCs were inoculated in the lower chamber. The nanoparticles in each treatment group were added into the tumor cells' chamber and incubated for 48 h. At the end of culture, tumor cells in the upper compartment were collected and the survival rate was evaluated by MTT. Lower chamber immune cells were collected and incubated with CD80-PE (ProteinTech, cat no. 14292-1-AP) (R-PE–conjugated Goat Anti-Rabbit IgG(H+L), ProteinTech, cat no. SA00008-2), CD86-FITC (ProteinTech, cat no. FITC-65068) and CD8-FITC (ProteinTech, cat no. FITC-65069), respectively. Flow cytometry was used to evaluate the degree of immune activation.

Distribution in vivo

All DOX in particles were labeled with FITC, and the same dose was given in the tail vein for each groups. IVIS (In Vivo Imaging System) spectral imaging system was used at 1 h, 2 h, 4 h, 8 h, 12 h and 24 h under the same parameters.

Construction of tumor model

Gastric adenocarcinoma cell line MFC was used to simulate the occurrence of gastric cancer. For vaccination of tumors, mice were weighed and randomly divided into different groups ($n \geq 5$), and all mice were injected with MFC cells (1×10^6) after a week of normal cultivation. After injection one week and all tumors reach to 10 mm in diameter, each mice were given drugs twice in 7 days, and the weight, tumor volume and survival rate were record every day. Three weeks later, all the surviving mice were dissected and the tumors were obtained and sectioned after measured. All tumor volumes were evaluated by the ellipsoid formula $V = \pi/6 \times L \times W^2$.

The killing progresses and malignancy degrees of tumor tissue were detected by hematoxylin and eosin (H&E) staining. The immune infiltration was demonstrated by CD8-FITC immunofluorescence staining. Tumor tissue was prepared into single cell suspension, CD80-PE and CD86-FITC immunofluorescence staining, and flow cytometry was used to analyze the activation of antigen-presenting cells in tumor tissue of mice. Blood was collected from the eyeball of the mice before death, and the concentration of cytokines was analyzed by ELISA.

Statistical analysis

All results were expressed as mean ± SD. For the single factor analysis, student t test was applied for two groups and the one way ANOVA was applied for multiple groups. All statistical analyses were performed by GraphPad prism software, and the $P < 0.05$ was considered as statistical significance.

Results

Synthesis and characterization of DOX@aiPS-DCexo

The synthesis diagram of the fusion system is shown in Fig. 1A. Firstly, DCs and iPSCs exosomes from the medium were extracted separately by super centrifugation, and the characteristic proteins of exosomes and functional proteins of maternal cells were been proved (Fig. 1B). Under the optimal fusion ratio of 3:2 (Fig. 1C), flow cytometry analysis of the convergence degree of the two fluorescence signals proved the successful fusion of the two exosomes (Fig. 1D). PD-1 antibody was combined with biotin to mediate antibody modification on membrane carriers with streptavidin (Fig. 1E), and the high expression of aPD-1 on the modified fusion vector was confirmed by Western blot analysis (Fig. 1F). Transmission electron microscopy (TEM) observation demonstrated the uniform shape of fusion carrier (Fig. 1G), and the hydration particle size with stable distribution at about 140 nm was detected by dynamic light scattering (DLS) (Fig. 1H). Then, DOX was uploaded into the nanovector as the chemotherapy drug. Compared with single exosome, the fusion vector owned higher encapsulation amount and loading rate (Fig. 1I, J), and the formed nanosystem presented stable drug release in the simulated in vivo environment and relatively violent release in the acidic environment (Fig. 1K).

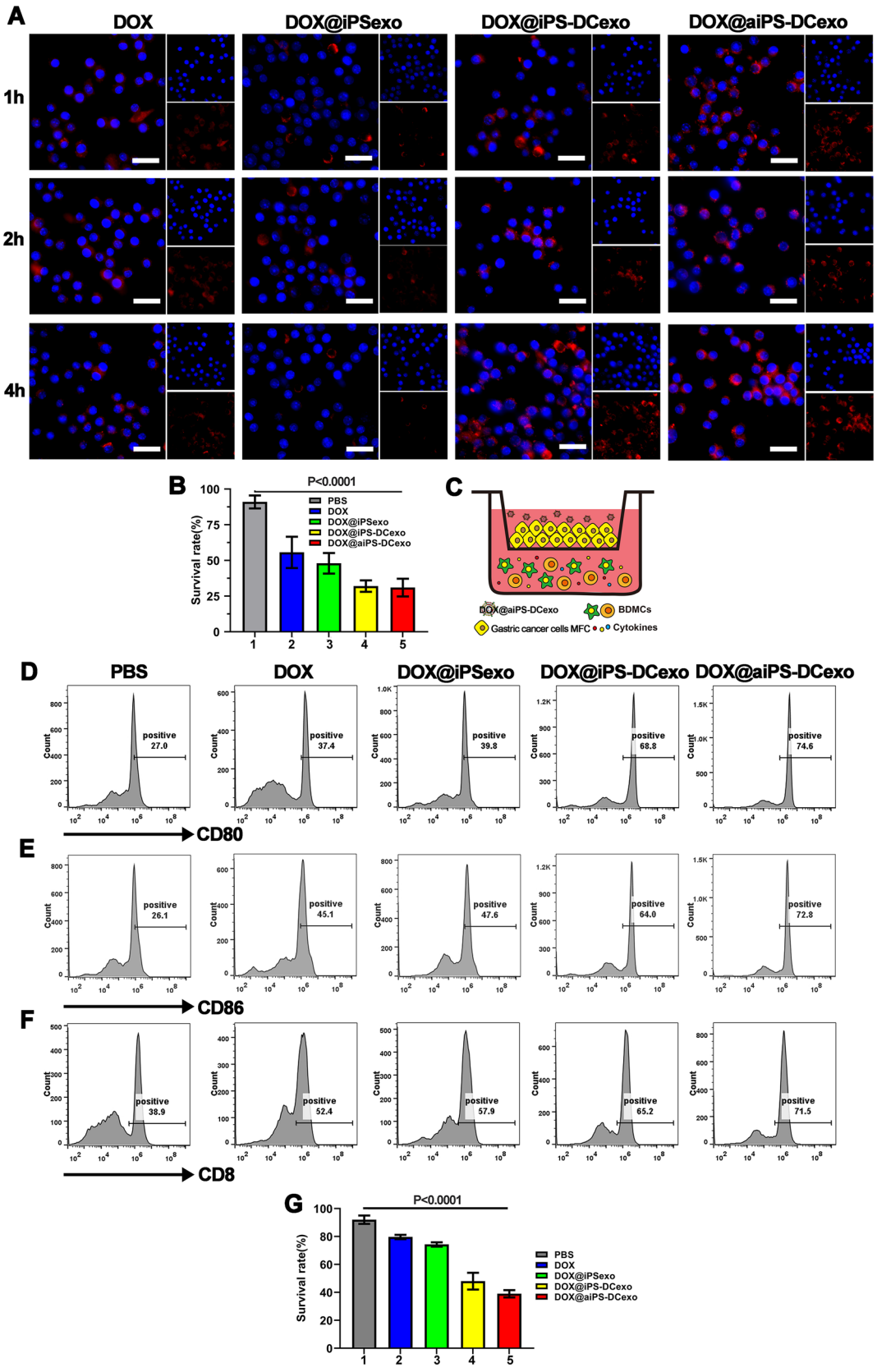
A
DOX
DOX@iPSexo
DOX@iPS-DCexo
DOX@aiPS-DCexo
1h
2h
4h
B
P<0.0001
PBS
DOX
DOX@iPSexo
DOX@iPS-DCexo
DOX@aiPS-DCexo
Survival rate(%)
C
DOX@aiPS-DCexo
BDMCs
Gastric cancer cells MFC
Cytokines
D
PBS
DOX
DOX@iPSexo
DOX@iPS-DCexo
DOX@aiPS-DCexo
positive 27.0
positive 37.4
positive 39.8
positive 68.8
positive 74.6
CD80
E
positive 26.1
positive 45.1
positive 47.6
positive 64.0
positive 72.8
CD86
F
positive 38.9
positive 52.4
positive 57.9
positive 65.2
positive 71.5
CD8
G
P<0.0001
Survival rate(%)
PBS
DOX
DOX@iPSexo
DOX@iPS-DCexo
DOX@aiPS-DCexo

◂**Fig. 2** Nanosystems attack tumor tissues through direct killing and immune activation. **A** Confocal microscopy observation in different groups of nanoparticles by RAW264.7 cells at different time points. Scale bars are 20 μm. **B** The survival rate of tumor cells after direct killing by the nanosystem. (**C**) Schematic diagram of transwell experiment. **D, E** Flow cytometry analyzer of the expression of CD80 and CD86 in the transwell system. **F** Flow cytometry analyzer of the activation of CD8+T cells in the lower lumen of transwell. **G** The survival rate of tumor cells after killing by the nanosystem in transwell. All data were expressed as mean ± SD. Statistical significance was calculated by one-way ANOVA with Tukey's post hoc test

Synergistic anti-tumor ability of chemotherapy and immunotherapy of DOX@aiPS-DCexo in vitro

Under the action of DCs exosomes, nanoparticles were significantly easier to be taken up by macrophages than those in the unfused group, and the fusion vector group increased the cellular uptake of drugs through the high DOX upload rate, and this increase would not be erased after the PD-1 antibody-modified vector (Fig. 2A). Chemotherapeutic drugs enable the nanosystem to demonstrate a strong killing ability of gastric cancer cells (Fig. 2B). To test synergistic immune stimulated effect under the combined therapy at the cellular level, Transwell experiment is performed as shown in Fig. 2C. Series of flow cytometry analysis showed that the DC cells in the system were heavily polarized (Fig. 2D, E), and cytotoxicity CD8+T cells widely proliferated (Fig. 2F), and tumor cell mortality obviously increased (Fig. 2G), which demonstrated the synergistic therapeutic effect of the nanosystem.

Distribution and biosafety of DOX@aiPS-DCexo in vivo

The biodistribution of several particles was analyzed in Institute of Cancer Research (ICR) mice, respectively. All

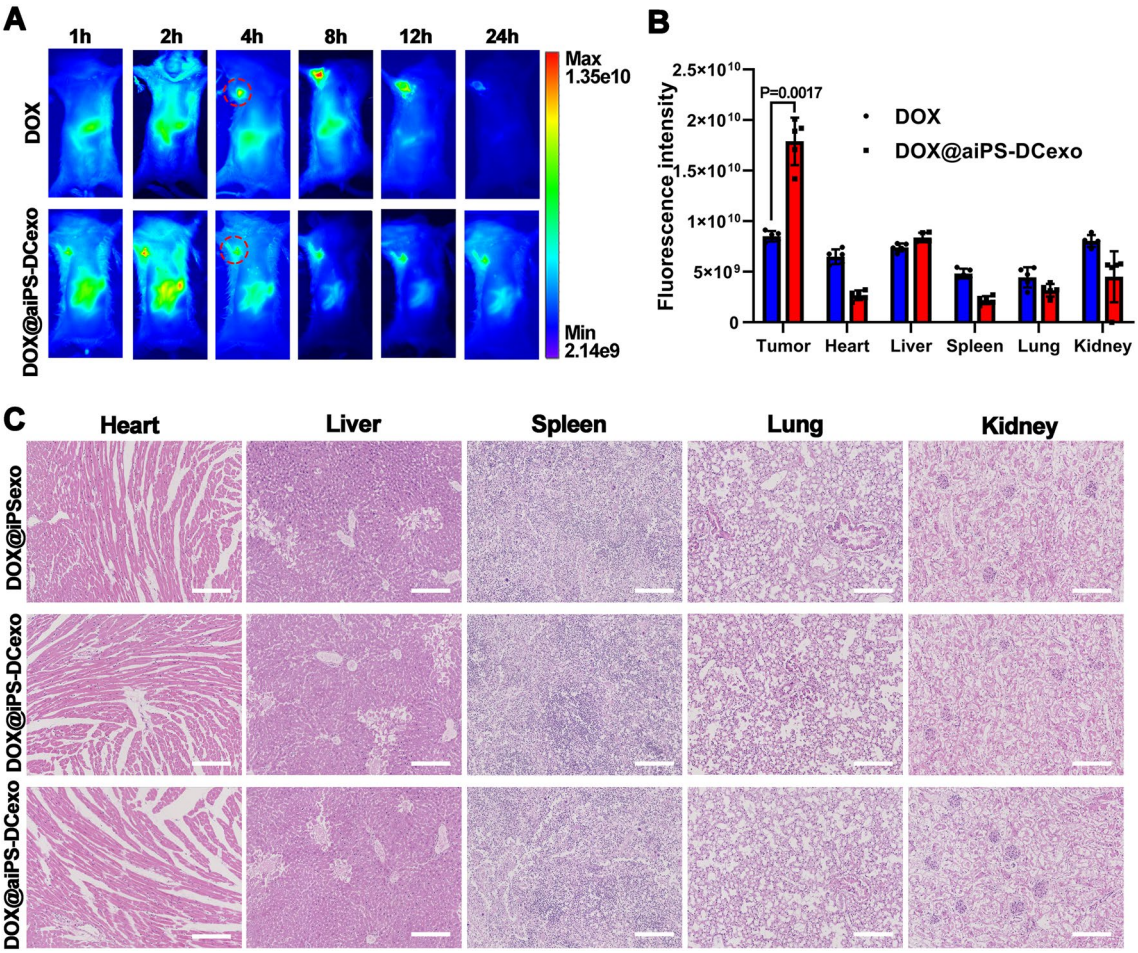

Fig. 3 In vivo tumor targeting and biosafety of nanosystems DOX@aiPS-DCexo. **A** IVIS observed metabolic distribution and tumor targeting in the nanosystem. Circles in red dotted line for sites of subcutaneous tumor inoculation. **B** Analysis of metabolism of nanosystem by fluorescence signal of organs in vivo. **C** HE staining of organ sections to analyze biosafety. Scale bars are 100 μm. All data were expressed as mean ± SD. Statistical significance was calculated by one-way ANOVA with Tukey's post hoc test

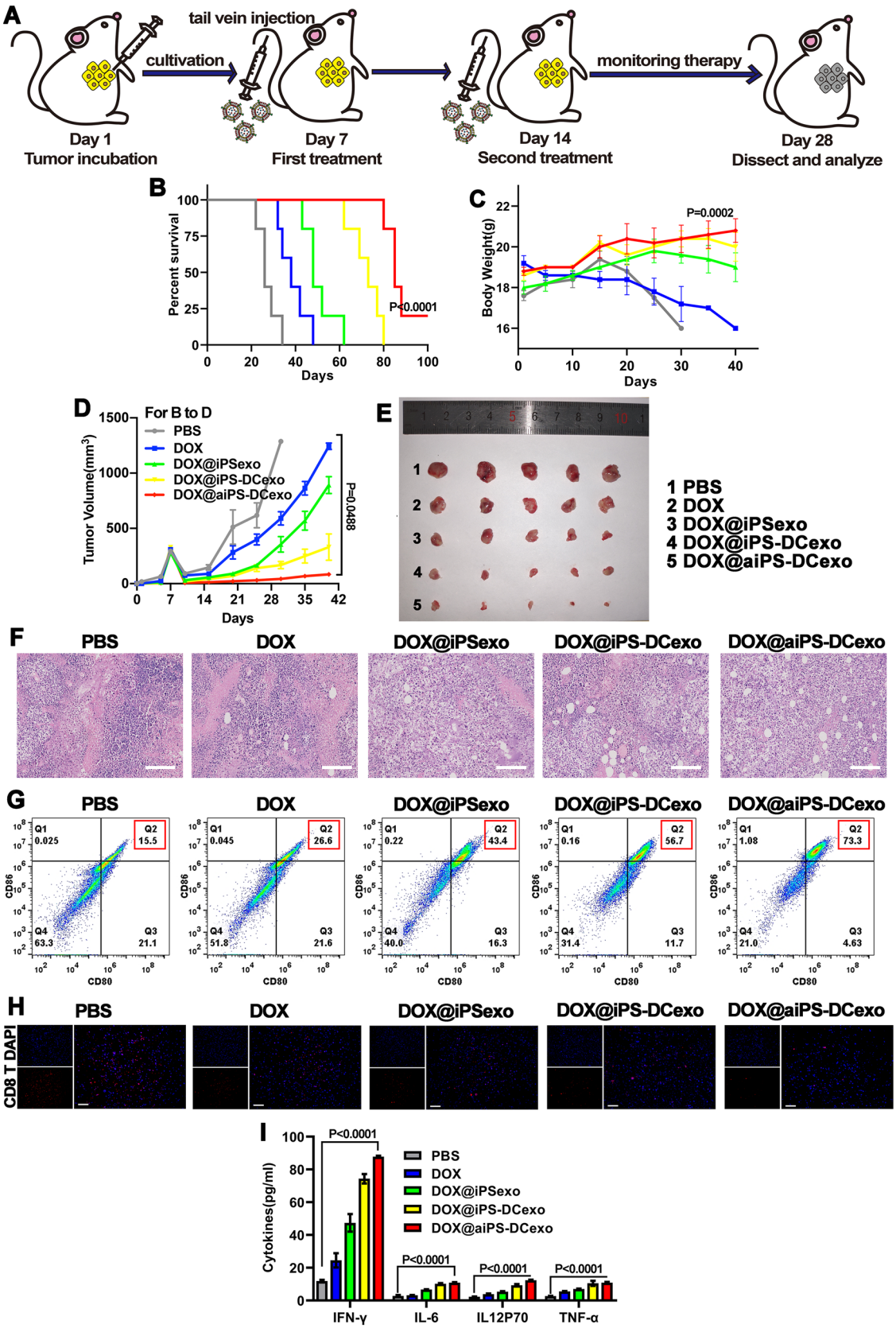
A
tail vein injection
cultivation
monitoring therapy
Day 1
Tumor incubation
Day 7
First treatment
Day 14
Second treatment
Day 28
Dissect and analyze
B
Percent survival
Days
P<0.0001
C
Body Weight(g)
Days
P=0.0002
D
For B to D
PBS
DOX
DOX@iPSexo
DOX@iPS-DCexo
DOX@aiPS-DCexo
Tumor Volume(mm3)
Days
P=0.0488
E
1 PBS
2 DOX
3 DOX@iPSexo
4 DOX@iPS-DCexo
5 DOX@aiPS-DCexo
F
PBS
DOX
DOX@iPSexo
DOX@iPS-DCexo
DOX@aiPS-DCexo
G
PBS
DOX
DOX@iPSexo
DOX@iPS-DCexo
DOX@aiPS-DCexo
CD86
CD80
Q1 0.025
Q2 15.5
Q4 63.3
Q3 21.1
Q1 0.045
Q2 26.6
Q4 51.8
Q3 21.6
Q1 0.22
Q2 43.4
Q4 40.0
Q3 16.3
Q1 0.16
Q2 56.7
Q4 31.4
Q3 11.7
Q1 1.08
Q2 73.3
Q4 21.0
Q3 4.63
H
PBS
DOX
DOX@iPSexo
DOX@iPS-DCexo
DOX@aiPS-DCexo
CD8 T DAPI
I
Cytokines(pg/ml)
P<0.0001
P<0.0001
P<0.0001
P<0.0001
PBS
DOX
DOX@iPSexo
DOX@iPS-DCexo
DOX@aiPS-DCexo
IFN-γ
IL-6
IL12P70
TNF-α

◂**Fig. 4** Construction of tumor model and investigation of tumor destructed capacity. **A** Schematic diagram of tumor model construction and treatment. Survival rate (**B**), body weights (**C**) and tumor volumes (**D**) of mice during treatment progress. **E** Photos of anatomical tumors at the end point of treatment. **F** H&E staining of tumor tissue sections. Scale bars are 100 μm. **G** Flow cytometry analyzer of the activation of dendritic cells in tumor tissue. **H** Confocal observation of tumor tissue CD8 T cells infiltration, red for CD8 T cells and DAPI for nucleus. **I** Changes of cytokine content in tumor interstitial fluid. All data were expressed as mean ± SD. Statistical significance was calculated by one-way ANOVA with Tukey's post hoc test

the particles presented fluorescence due to the DOX labeled with fluorescent dye FITC, and the fluorescence signal was detected by the IVIS system. The nanosystem DOX@aiPS-DCexo accumulated in tumor tissue 1 h after injection, by contrast, group without iPS-exo failed in the tumor target (Fig. 3A). The comparison of fluorescence signal quantization in each organ also proved that the nanosystem DOX@aiPS-DCexo tend to accumulate in tumors rather than major organs (Fig. 3B). At the same time, the nanosystem DOX@aiPS-DCexo injected through the tail vein would not produce organotoxicity to the major organs heart, liver, spleen, lung, spleen, which proved the feasibility of the safe application of nanoparticles in vivo (Fig. 3C).

Anti-tumor capabilities of the nanosystems DOX@aiPS-DCexo

The anti-tumor capacity of the nanosystem was tested in the subcutaneous tumor model formed by the gastric adenocarcinoma cells MFC, the strategy of tumor implantation and treatment are shown in Fig. 4A. Compared with the PBS group, the fusion system DOX@aiPS-DCexo currently suppressed the process of tumor expansion, prolonged the survival rates and kept the stable weight (Fig. 4B–D), and this inhibitory effect could be more clearly reflected by dissecting the tumor of mice at the end point of treatment (Fig. 4E). H&E staining of tumor tissue sections visually presented the destruction of tumor tissue by chemotherapy drugs and the improvement of malignant degree of tumor tissue by immunotherapy (Fig. 4F). In the analysis of tumor tissue immune microenvironment, we found that DC-exos fusion group could effectively recruit dendritic cells and stimulate their mature differentiation (Fig. 4G), and with the assistant of aPD-1, the tissue infiltration of cytotoxic CD8+T cells was greatly increased (Fig. 4H). A consistent pattern of cytokine changes also demonstrated the immune activation (Fig. 4I). In conclusion, the fusion system DOX@aiPS-DCexo efficiently inhibits tumor growth through synergistic chemotherapy and immunotherapy.

Discussions and conclusions

In recent years, exosomes have been gradually applied in clinical oncology therapy in the form of targeted drug delivery or anti-tumor therapy. iPSCs are pluripotent stem cells generated by the reprogramming of somatic cells, widely used in organ transplantation and disease treatment for the available source, ethical safety and integrated characteristics of stem cells. iPSCs exosomes were confirmed to possess tumor tissue targeting capacity mediated by the CXCR4/SDR1 axis, and this targeting ability is confirmed in Fig. 3A. Moreover, its content substances can significantly inhibit the proliferation and differentiation of gastric cancer stem cells, effectively prevent the remodeling of tumor tissues and inhibit the recurrence of tumors. However, the direct killing ability of iPSCs exosomes was not efficient enough to destroy the formed tumor tissue and requires further combination with tumor tissue injury treatment, making them more suitable for application as the functional targeted delivery vectors for anti-tumor drugs.

Tumor immunotherapy is an important synergistic means of chemotherapy, but the effect of immunotherapy is limited by the characteristics of tumor hypoxic microenvironment, such as less infiltration of immune cells and loss of cytotoxicity due to lymphocyte suppression. Dendritic cells' exosomes have been proved to be effective in recruiting immune cells to gather at the tumor site, stimulating the mature differentiation of antigen-presenting cells and facilitating the presentation of tumor-associated antigens to downstream lymphocytes to generate a series of anti-tumor immune responses. This immune-enhancing effect was further amplified by lifting immunosuppression of lymphocytes by vector-modified with PD-1 antibody. Therefore, by fusion vector based on iPSCs exosomes with DCs exosomes and modified with aPD-1, and the functional fusion vector aiPS-DCexo could provide the targeted delivery for anti-tumor drugs to tumor tissues and enhance the efficacy of tumor immunotherapy. The immune stimulation effect of fusion vectors was well demonstrated in Transwell experiments (Fig. 2C–G).

Chemotherapeutic drugs play an important role in the clinical treatment of gastric cancer and other tumors which are difficult to be surgically resected. However, most chemotherapeutic drugs seriously affect the quality of life of patients due to their low efficacy and high organ toxicity. Utilizing fusion vector aiPS-DCexo as targeted delivery vector of chemotherapy drugs can efficaciously inhibit tumor expansion, ensure the weight of tumor-bearing mice and increase the survival rate of mice due to weakened organ toxicity (Fig. 4).

The poor prognosis of chemotherapy is also an urgent problem that needs to be solved in tumor clinical treatment. Even if the tumor tissue is damaged temporarily, the tumor stem cells will proliferate and differentiate into recurrent tumors. The introduction of iPSCs exosomes can particularly inhibit the

proliferation of tumor stem cells and prevent tumor remodeling. At the same time, the massive exposure of tumor associated antigens after the action of chemotherapeutic drugs provides an opportunity for the immune response. After DC-exos recruits and infiltrate lots of immune cells, the efficient anti-tumor immune response can remove the "garbage" substances generated after tumor necrosis and promote a large number of memory immune cells, completely eliminating the risk of recurrence.

In summary, in this study, we fused iPSCs exosomes with DCs exosomes, modified with aPD-1, and uploaded DOX to manufacture a gastric cancer targeted killing system DOX@aiPS-DCexo for synergistic chemotherapy and immunotherapy. In the exploration of gastric adenocarcinoma MFC solid tumor model, nanoparticles DOX@aiPS-DCexo targeted accumulate in tumor tissues in vivo, destroyed tumor structure and exposed a mass of tumor-associated antigens, then recruited immune cells to infiltrate and removed the inhibition of cytotoxic CD8+T cells, which amplifying the anti-tumor immune response layer by layer, realizing the synergistic effect of immunotherapy on chemotherapy and improving the odious prognosis of gastric cancer. Combined with the characteristics of availability of raw materials, good biocompatibility and no organ toxicity in vivo, the nanosystem is suitable to be applied as the carrier for multiple anti-tumor chemotherapy drugs to achieve accurate delivery and synergistic treatment, or be applied in the prognosis of surgical treatment, with the broad clinical application prospects.

Acknowledgements Not applicable.

Author Contributions YL, LT, TZ and JZ conceived the project. YL and LT performed the experiments and analyzed the results. YL, TZ and JZ provided useful suggestions to this work. YL, LT, TZ and JZ wrote the manuscript.

Availability of data and materials The datasets in the current study are included in the published article or available from the corresponding author on reasonable request.

Declarations

Conflict of interest The authors declare no competing financial interest.

Ethics approval and consent to participate All animal studies complied with the China National Institute's Guidelines on the Care and Use of Laboratory and were performed according to National Institute of Health (NIH) Guide and approved by the Laboratory Animal Management Committee of Jilin University.

Consent for publication Not applicable.

References

1. Wagner AD, Syn NLX, Moehler M et al (2017) Chemotherapy for advanced gastric cancer. Cochrane database Syst Rev. https://doi.org/10.1002/14651858.CD004064.PUB4
2. Joshi SS, Badgwell BD (2021) Current treatment and recent progress in gastric cancer. CA Cancer J Clin 71:264–279. https://doi.org/10.3322/CAAC.21657
3. Thrift AP, El-Serag HB (2020) Burden of gastric cancer. Clin Gastroenterol Hepatol 18:534–542. https://doi.org/10.1016/J.CGH.2019.07.045
4. Wang A, Li Z, Wang M et al (2020) Molecular characteristics of synchronous multiple gastric cancer. Theranostics 10:5489–5500. https://doi.org/10.7150/THNO.42814
5. Moss SF (2017) The clinical evidence linking helicobacter pylori to gastric cancer. CMGH 3:183–191. https://doi.org/10.1016/J.JCMGH.2016.12.001
6. Sa JK, Hong JY, Lee IK et al (2020) Comprehensive pharmacogenomic characterization of gastric cancer. Genome Med. https://doi.org/10.1186/S13073-020-0717-8
7. Diaz-Nieto R, Orti-Rodríguez R, Winslet M (2013) Post-surgical chemotherapy versus surgery alone for resectable gastric cancer. Cochrane database Syst Rev. https://doi.org/10.1002/14651858.CD008415.PUB2
8. Stewart OA, Wu F, Chen Y (2020) The role of gastric microbiota in gastric cancer. Gut Microbes 11:1220–1230. https://doi.org/10.1080/19490976.2020.1762520
9. Li R, Hou WH, Chao J et al (2018) Chemoradiation improves survival compared with chemotherapy alone in unresected nonmetastatic gastric cancer. J Natl Compr Cancer Netw 16:950–958. https://doi.org/10.6004/JNCCN.2018.7030
10. Carmona-Bayonas A, Jiménez-Fonseca P, Lorenzo MLS et al (2016) On the effect of triplet or doublet chemotherapy in advanced gastric cancer: results from a national cancer registry. J Natl Compr Cancer Netw 14:1379–1388. https://doi.org/10.6004/JNCCN.2016.0148
11. Wang F, Porter M, Konstantopoulos A et al (2017) Preclinical development of drug delivery systems for paclitaxel-based cancer chemotherapy. J Control Release 267:100–118. https://doi.org/10.1016/J.JCONREL.2017.09.026
12. Shafabakhsh R, Yousefi B, Asemi Z et al (2020) Chitosan: a compound for drug delivery system in gastric cancer-a review. Carbohydr Polym. https://doi.org/10.1016/J.CARBPOL.2020.116403
13. Li K, Zhang A, Li X et al (2021) Advances in clinical immunotherapy for gastric cancer. Biochim Biophys Acta Rev Cancer. https://doi.org/10.1016/J.BBCAN.2021.188615
14. Hußtegge M, Hoang NA, Rebstock J et al (2021) PD-1 inhibition in patient derived tissue cultures of human gastric and gastroesophageal adenocarcinoma. Oncoimmunology. https://doi.org/10.1080/2162402X.2021.1960729
15. Li Q, Zhou ZW, Lu J et al (2022) PD-L1 P146R is prognostic and a negative predictor of response to immunotherapy in gastric cancer. Mol Ther 30:621–631. https://doi.org/10.1016/J.YMTHE.2021.09.013
16. Umeda S, Kanda M, Shimizu D et al (2022) Lysosomal-associated membrane protein family member 5 promotes the metastatic potential of gastric cancer cells. Gastric Cancer. https://doi.org/10.1007/S10120-022-01284-Y
17. Kamada T, Togashi Y, Tay C et al (2019) PD-1+ regulatory T cells amplified by PD-1 blockade promote hyperprogression of cancer. Proc Natl Acad Sci USA 116:9999–10008. https://doi.org/10.1073/PNAS.1822001116/-/DCSUPPLEMENTAL
18. Hu X, Wang J, Chu M et al (2021) Emerging Role of ubiquitination in the Regulation of PD-1/PD-L1 in Cancer Immunotherapy. Mol Ther 29:908–919. https://doi.org/10.1016/J.YMTHE.2020.12.032
19. Li C, Ruan J, Yang M et al (2015) Human induced pluripotent stem cells labeled with fluorescent magnetic nanoparticles for targeted imaging and hyperthermia therapy for gastric cancer. Cancer Biol Med 12:163–174. https://doi.org/10.7497/J.ISSN.2095-3941.2015.0040
20. Ehtesham M, Yuan X, Kabos P et al (2004) Glioma tropic neural stem cells consist of astrocytic precursors and their migratory capacity is mediated by CXCR4. Neoplasia 6:287–293. https://doi.org/10.1593/NEO.3427

21. Molyneaux KA, Zinszner H, Kunwar PS et al (2003) The chemokine SDF1/CXCL12 and its receptor CXCR4 regulate mouse germ cell migration and survival. Development 130:4279–4286. https://doi.org/10.1242/DEV.00640
22. Ceradini DJ, Kulkarni AR, Callaghan MJ et al (2004) Progenitor cell trafficking is regulated by hypoxic gradients through HIF-1 induction of SDF-1. Nat Med 10:858–864. https://doi.org/10.1038/NM1075
23. Lee EX, Lam DH, Wu C et al (2011) Glioma gene therapy using induced pluripotent stem cell derived neural stem cells. Mol Pharm 8:1515–1524. https://doi.org/10.1021/MP200127U
24. Yang J, Lam DH, Goh SS et al (2012) Tumor tropism of intravenously injected human-induced pluripotent stem cell-derived neural stem cells and their gene therapy application in a metastatic breast cancer model. Stem Cells 30:1021–1029. https://doi.org/10.1002/STEM.1051
25. Koizumi S, Gu C, Amano S et al (2011) Migration of mouse-induced pluripotent stem cells to glioma-conditioned medium is mediated by tumor-associated specific growth factors. Oncol Lett 2:283–288. https://doi.org/10.3892/OL.2011.234
26. Li W, Zhang X, Wu F et al (2019) Gastric cancer-derived mesenchymal stromal cells trigger M2 macrophage polarization that promotes metastasis and EMT in gastric cancer. Cell Death Dis. https://doi.org/10.1038/S41419-019-2131-Y
27. Gao W, Liu H, Yuan J et al (2016) Exosomes derived from mature dendritic cells increase endothelial inflammation and atherosclerosis via membrane TNF-α mediated NF-κB pathway. J Cell Mol Med 20:2318–2327. https://doi.org/10.1111/JCMM.12923
28. Fu C, Zhou L, Mi QS, Jiang A (2020) Dc-based vaccines for cancer immunotherapy. Vaccines 8:1–16. https://doi.org/10.3390/VACCINES8040706
29. Pitt JM, André F, Amigorena S et al (2016) Dendritic cell-derived exosomes for cancer therapy. J Clin Invest 126:1224–1232. https://doi.org/10.1172/JCI81137
30. Yao Y, Fu C, Zhou L et al (2021) Dc-derived exosomes for cancer immunotherapy. Cancers (Basel). https://doi.org/10.3390/CANCERS13153667
31. Familtseva A, Jeremic N, Tyagi SC (2019) Exosomes: cell-created drug delivery systems. Mol Cell Biochem. https://doi.org/10.1007/S11010-019-03545-4
32. Liang Y, Duan L, Lu J, Xia J (2021) Engineering exosomes for targeted drug delivery. Theranostics 11:3183–3195. https://doi.org/10.7150/THNO.52570
33. Zhong H, Yang Y, Ma S et al (2011) Induction of a tumour-specific CTL response by exosomes isolated from heat-treated malignant ascites of gastric cancer patients. Int J Hyperth 27:604–611. https://doi.org/10.3109/02656736.2011.564598
34. Liu J, Ren L, Li S et al (2021) The biology, function, and applications of exosomes in cancer. Acta Pharm Sin B 11:2783–2797. https://doi.org/10.1016/J.APSB.2021.01.001
35. Chai Z, Ran D, Lu L et al (2019) Ligand-modified cell membrane enables the targeted delivery of drug nanocrystals to glioma. ACS Nano. https://doi.org/10.1021/ACSNANO.9B00661
36. Song X, Jiang Y, Zhang W et al (2022) Transcutaneous tumor vaccination combined with anti-programmed death-1 monoclonal antibody treatment produces a synergistic antitumor effect. Acta Biomater 140:247–260. https://doi.org/10.1016/j.actbio.2021.11.033
37. Jiang M, Chen W, Yu W et al (2021) Sequentially pH-responsive drug-delivery nanosystem for tumor immunogenic cell death and cooperating with immune checkpoint blockade for efficient cancer chemoimmunotherapy. ACS Appl Mater Interfaces 13:43963–43974. https://doi.org/10.1021/acsami.1c10643
38. Shao J, Zaro J, Shen Y (2020) Advances in exosome-based drug delivery and tumor targeting: from tissue distribution to intracellular fate. Int J Nanomed 15:9355–9371. https://doi.org/10.2147/IJN.S281890
39. Wang S, Ping M, Song B et al (2020) Exosomal circPRRX1 enhances doxorubicin resistance in gastric cancer by regulating mir-3064-5p/PTPN14 signaling. Yonsei Med J 61:750–761. https://doi.org/10.3349/YMJ.2020.61.9.750
40. Razavi SMS, Vaziri RM, Karimi G et al (2020) Crocin increases gastric cancer cells' sensitivity to doxorubicin. Asian Pacific J Cancer Prev 21:1959–1967. https://doi.org/10.31557/APJCP.2020.21.7.1959
41. Xu J, Liu D, Niu H et al (2017) Resveratrol reverses doxorubicin resistance by inhibiting epithelial-mesenchymal transition (EMT) through modulating PTEN/Akt signaling pathway in gastric cancer. J Exp Clin Cancer Res. https://doi.org/10.1186/S13046-016-0487-8

Authors and Affiliations

Yezhou Li[3] · Leilei Tian[4] · Tiancheng Zhao[2] · Jiayu Zhang[1]

✉ Tiancheng Zhao
zhaotiancheng@jlu.edu.cn

✉ Jiayu Zhang
zhangjiayu@jlu.edu.cn

[1] Department of Gastrointestinal Colorectal and Anal Surgery, China-Japan Union Hospital of Jilin University, Changchun 130033, Jilin, China

[2] Department of Endoscopy Center, China-Japan Union Hospital of Jilin University, Changchun 130033, Jilin, China

[3] Department of Vascular Surgery, China-Japan Union Hospital of Jilin University, Changchun 130033, Jilin, China

[4] Department of Operating Room, China-Japan Union Hospital of Jilin University, Changchun 130033, Jilin, China